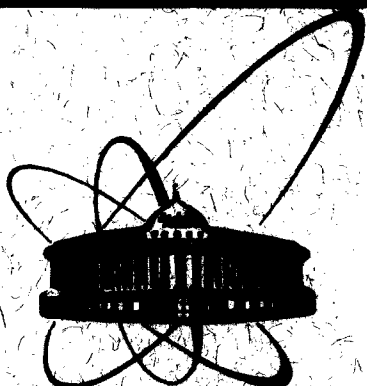


89-780



СООБЩЕНИЯ
ОБЪЕДИНЕННОГО
ИНСТИТУТА
ЯДЕРНЫХ
ИССЛЕДОВАНИЙ
ДУБНА

E 27

E2-89-780

G. V. Efimov, M. A. Ivanov, S. G. Mashnik*

$\pi\pi$ -SCATTERING
IN THE QUARK CONFINEMENT MODEL.
PHASE SHIFTS

* Institute of Applied Physics, Kishinev, USSR

1989

1. INTRODUCTION

The $\pi\pi$ -scattering plays a specific role in the particle physics. On the one hand, because of the absence of pion targets experimental data on the $\pi\pi$ -scattering are obtained in an indirect way from other reactions with pions: $\pi N \rightarrow N\pi\pi$, K_{l4} -decay, $e^+e^- \rightarrow \pi\pi$, $NN \rightarrow 2\pi$, $K \rightarrow 2\pi(3\pi)$, $\eta \rightarrow 3\pi$ etc. (see, for example [1]-[4]).

To extrapolate the experimental data to the small energies, various theoretical models are used which sometimes lead to uncertainties in the final results. Therefore, it is necessary to perform the theoretical investigations for the real understanding of such processes and, in particular, to develop models providing certain quantitative predictions.

On the other hand, the $\pi\pi$ -scattering has a number of specific features: it is the simplest system of spinless particles; a pion is the lightest hadron; the $\pi\pi$ -amplitudes are the complete cross-symmetrical ones. As a rule, the parameters of any model are very sensitive to description on the experimental data of the $\pi\pi$ -scattering so the latter can be considered as a good test for the models.

Theoretically, the $\pi\pi$ -scattering has been investigated in many approaches: dispersional relations, chiral-broken theory, current algebra, duality models and quark ones. The good classifications of the models suggested up to the middle of 1975 year are given in the book [1]. The models suggested later are adequately described in [2]. The complete review of this problem can be found in [1]-[4]. It should be remarked that any theoretical approach claiming to describe strong interactions has to explain the $\pi\pi$ -scattering as the latter is included as a part in more complicated processes (see, for example, [3]). As a rule, the $\pi\pi$ -scattering was considered disregarding the quark structure of pions and intermediate mesons (for example, dispersional relations, chiral theory, current algebra). At present, much attention is paid to the study of quark degrees of freedom in the hadron-hadron scattering at low energies. Therefore, it is interesting to investigate how the quark structure of mesons manifests itself in the $\pi\pi$ -scattering.

In the paper [5], the QCM was suggested to describe the hadron quark structure at low energies with allowance for the quark confinement. Both the static hadron characteristics such as decay widths, magnetic moments etc. and the electromagnetic and strong form factors were described in the framework of this model with quite a good accuracy [5]-[9].

The aim of this work is the description of the $\pi\pi$ -scattering in the QCM and the investigation of the stability of the final results to a change of input model parameters. Especially, we are interested in the nature of the broad scalar $\epsilon(700-800)$ -resonance. Our conclusion consists in that the experimental data of the s-wave $\pi\pi$ -scattering cannot be described without including this resonance.

2. THE BASIC NOTIONS OF THE QCM. KINEMATICS AND NOTATION

The QCM was described in details in [5]. Here, we proceed with the basic notions of this model. In the QCM, hadrons are considered to be collective colourless excitations of the quark-gluon interactions. The confinement is supposed to be realized as averaging over some vacuum gluon backgrounds.

The quark diagrams describing hadron interactions are induced by the S-matrix which can be written as

$$S = \int d\sigma_{vac} T \exp\{i \int d^4x L_I(x)\}. \quad (1)$$

Here, L_I is the Lagrangian describing an interaction of quarks with hadrons. The time-ordered product is supposed to be the ordinary Wick T-product of hadron and quark fields with the quark propagator:

$$\begin{aligned} & \langle 0 | T \{ q_f^a(x) \bar{q}_{f'}^{a'}(x') \} | 0 \rangle = \\ & \delta_{f'f} \delta_{a'a} (i\hat{\partial} + B_{vac})^{-1} \delta(x - x') = \delta_{f'f} \delta_{a'a} S(x, x' | B_{vac}). \end{aligned}$$

The quark fields must be equal to zero after normal ordering.

The measure $d\sigma_{vac}$, i.e. the way of averaging of quark diagrams over vacuum gluon backgrounds is defined as [5]:

$$\begin{aligned} & \int d\sigma_{vac} \text{tr} [M(x_1) S(x_1, x_2 | B_{vac}) \dots M(x_n) S(x_n, x_1 | B_{vac})] \Rightarrow \\ & \Rightarrow \int d\sigma_\lambda \text{tr} [M(x_1) S_\lambda(x_1 - x_2) \dots M(x_n) S_\lambda(x_n - x_1)], \end{aligned}$$

where

$$S_\lambda(x_1 - x_2) = \int \frac{d^4p}{(2\pi)^4 i} \frac{e^{-ip(x_1 - x_2)}}{\lambda \Lambda_f - \hat{p}}$$

The mass dimensional parameter Λ_f defines the confinement region of quarks with flavour f .

The integration measure $d\sigma_\lambda$ is defined as

$$\int \frac{d\sigma_\lambda}{\lambda - z} = G(z) = a(-z^2) + zb(-z^2),$$

where $G(z)$ is called the confinement function. The shape of $G(z)$ is yet unknown and choice is one of the model assumptions.

Here, we use the functions $a(u)$ and $b(u)$ obtained in [5]:

$$a(u) = 2 \exp\{-u^2 - u\}, \quad (2)$$

$$b(u) = 2 \exp\{-u^2 + 0.4u\}.$$

The mass dimensional parameters are equal to

$$\Lambda_u = \Lambda_d \equiv \Lambda = 460 \text{ Mev} \quad \Lambda_s = 506 \text{ Mev}.$$

In the QCM, all calculations of physical matrix elements are based on the $1/N_c$ -expansion [5]. The low-energy $\pi\pi$ -scattering in the lowest order in $1/N_c$ -expansion is described by the diagrams in Fig.1

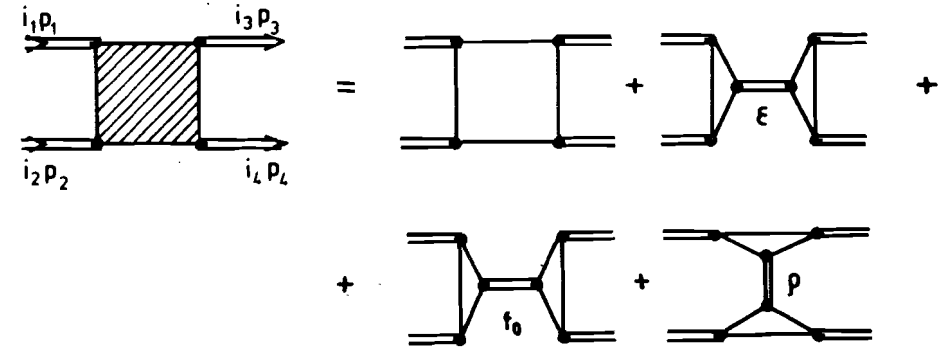


Fig.1. The diagrams defining the low-energy $\pi\pi$ -scattering in one-loop approximation (zero-order on $1/N_c$ -expansion).

Let us choose the meson-quark interaction Lagrangian in the following form [5],[7]

$$L_I^M = \frac{gM}{\sqrt{2}} \sum_{i=0}^8 M_i \bar{q} \Gamma_M \lambda^i q. \quad (3)$$

Here, M_i are the Euclidean fields connected with the physical ones in a standard manner [5], λ_i are the Gell-Mann matrices ($\lambda^0 = \sqrt{\frac{2}{3}}I$), Γ_M are the correspondent Dirac matrices: $i\gamma_5$ for the pseudoscalar mesons ($P = \pi$), γ_μ for the vector ones ($V = \rho, \omega$), $I - i\frac{H}{\Lambda}\hat{\partial}$ for the scalar ones ($S = \epsilon; f_0$). The role of the auxiliary term with a derivative in the scalar meson quark current will be discussed in detail lately.

The mixing angles are defined in a standard manner

$$\epsilon \rightarrow \cos(\delta_S) \frac{\bar{u}u + \bar{d}d}{\sqrt{2}} - \sin(\delta_S) \bar{s}s; \quad (4)$$

$$f_0 \rightarrow -\sin(\delta_S) \frac{\bar{u}u + \bar{d}d}{\sqrt{2}} - \cos(\delta_S) \bar{s}s;$$

$$\delta_S = \theta_S - \theta_I, \quad \sin(\theta_I) = \frac{1}{\sqrt{3}}.$$

The coupling constants g_M are defined by the compositeness condition implying that the wave function renormalization constant of meson M is equal to zero [10]

$$Z_M = 1 + g_M^2 \tilde{\Pi}'_M(m_M^2) = 0, \quad (5)$$

where $\tilde{\Pi}_M(p_M^2)$ is the mass operator of the meson M. The compositeness condition (5) implies that only mesonic degrees of freedom are independent in the meson-quark system describing by the interaction Lagrangian (3) and quarks appear as auxiliary virtual particles defining the hadron interactions. Thus, quarks allow one to describe the hadron inner structure. From the point of view of the quark-hadron duality we are in the hadron sector and quarks in the Lagrangian (3) are constituents and cannot appear in the observable hadron spectrum.

It is more convenient to use the effective coupling constants $h_M = 3g_M^2/4\pi^2$ under calculations instead of g_M . Their expressions and numerical values are given in Appendix 1. We will use below the following notation: $C_A^{(n)} = \int_0^\infty dt t^n a(t)$; $C_B^{(n)} = \int_0^\infty dt t^n b(t)$; $x_M = (m_M/\Lambda)^2$; $y_M = (m_M/\Lambda_s)^2$, where m_M is the meson mass.

Let us define our terminology and notation which we will use further. The $\pi\pi$ -scattering amplitude is defined in a standard manner (see, for example [1],[2]):

$$\begin{aligned} & \langle p_3 i_3; p_4 i_4 | S - I | p_1 i_1; p_2 i_2 \rangle = \quad (6) \\ & = \frac{i(2\pi)^4 \delta^{(4)}(p_1 + p_2 - p_3 - p_4)}{(2\pi)^{64} \sqrt{p_1^0 p_2^0 p_3^0 p_4^0}} M_{inv}^{i_3 i_4, i_1 i_2}(s, t, u) = \\ & = \frac{2i\delta^{(4)}(p_1 + p_2 - p_3 - p_4)}{\pi \sqrt{p_1^0 p_2^0 p_3^0 p_4^0}} [A(s, t, u) \delta_{i_1 i_2} \delta_{i_3 i_4} + \\ & \quad + A(t, s, u) \delta_{i_1 i_3} \delta_{i_2 i_4} + A(u, t, s) \delta_{i_1 i_4} \delta_{i_2 i_3}], \end{aligned}$$

where p_j and i_j are momenta and isospin indices, respectively; s, t, u are the Mandelstam variables: $s = (p_1 + p_2)^2$, $t = (p_1 - p_3)^2$, $u = (p_1 - p_4)^2$.

After standard calculations [5] of the matrix elements corresponding to the diagrams in Fig.1 one can obtain

$$\begin{aligned} A(s, t, u) & = \frac{1}{32\pi} \{-G_{box}(s, t, u) + G_{\epsilon\pi\pi}^2(s) D_\epsilon(s) + G_{f_0\pi\pi}^2(s) D_{f_0}(s)\} \quad (7) \\ & \quad + (s-u) G_{\rho\pi\pi}^2(t) D_\rho(t) + (s-t) G_{\rho\pi\pi}^2(u) D_\rho(u). \end{aligned}$$

Here, $D_{\epsilon, f_0, \rho}$ are the propagators of the ϵ, f_0 and ρ -mesons, respectively:

$$D_S(p_S^2) = h_S \tilde{D}_S(p_S^2) = \quad (8)$$

$$= \frac{h_S}{\Pi_S(p_S^2) - \Pi_S(m_S^2)} = \frac{2}{m_S^2 R(x_S) - w_S R(w_S)},$$

$$D_\rho(p_\rho^2) = h_\rho \tilde{D}_\rho(p_\rho^2) = \quad (9)$$

$$= \frac{h_\rho}{\Pi_\rho(p_\rho^2) - \Pi_\rho(m_\rho^2)} = \frac{3}{m_\rho^2 B_0(x_\rho) - w_\rho B_0(w_\rho)},$$

where Π_M is the meson M mass operator and $w_M = (p_M/\Lambda)^2$. The functions G_{box} , $G_{\epsilon\pi\pi}$, $G_{f_0\pi\pi}$, $G_{\rho\pi\pi}$, R and B_0 are given in Appendix 2.

The $\pi\pi$ -scattering amplitudes with isospin I are defined as

$$\begin{aligned} A^0(s, t, u) & = 3A(s, t, u) + A(t, s, u) + A(u, t, s) = \quad (10) \\ & = \frac{1}{32\pi} \{-[3G_{box}(s, t, u) + G_{box}(t, s, u) + G_{box}(u, t, s)] + \end{aligned}$$

$$\begin{aligned}
& + [3G_{\epsilon\pi\pi}^2(s)D_\epsilon(s) + G_{\epsilon\pi\pi}^2(t)D_\epsilon(t) + G_{\epsilon\pi\pi}^2(u)D_\epsilon(u)] + \\
& + [3G_{f_0\pi\pi}^2(s)D_{f_0}(s) + G_{f_0\pi\pi}^2(t)D_{f_0}(t) + G_{f_0\pi\pi}^2(u)D_{f_0}(u)] + \\
& + [(s-u)G_{\rho\pi\pi}^2(t)D_\rho(t) + (s-t)G_{\rho\pi\pi}^2(u)D_\rho(u)] = \\
& = A_{\text{box}}^0(s, t, u) + A_\epsilon^0(s, t, u) + A_{f_0}^0(s, t, u) + A_\rho^0(s, t, u); \\
A^1(s, t, u) & = A(t, s, u) - A(u, t, s) = \tag{11}
\end{aligned}$$

$$\begin{aligned}
& = \frac{1}{32\pi} \{-[G_{\text{box}}(t, s, u) - G_{\text{box}}(u, t, s)] + \\
& + [G_{\epsilon\pi\pi}^2(t)D_\epsilon(t) - G_{\epsilon\pi\pi}^2(u)D_\epsilon(u)] + \\
& + [G_{f_0\pi\pi}^2(t)D_{f_0}(t) - G_{f_0\pi\pi}^2(u)D_{f_0}(u)] + \\
& + [(s-u)G_{\rho\pi\pi}^2(t)D_\rho(t) - (s-t)G_{\rho\pi\pi}^2(u)D_\rho(u) + \\
& + 2(t-u)G_{\rho\pi\pi}^2(s)D_\rho(s)]\} = \\
& = A_{\text{box}}^1(s, t, u) + A_\epsilon^1(s, t, u) + A_{f_0}^1(s, t, u) + A_\rho^1(s, t, u); \\
A^2(s, t, u) & = A(t, s, u) + A(u, t, s) = \tag{12} \\
& = \frac{1}{32\pi} \{-[G_{\text{box}}(t, s, u) + G_{\text{box}}(u, t, s)] + \\
& + [G_{\epsilon\pi\pi}^2(t)D_\epsilon(t) + G_{\epsilon\pi\pi}^2(u)D_\epsilon(u)] + \\
& + [G_{f_0\pi\pi}^2(t)D_{f_0}(t) + G_{f_0\pi\pi}^2(u)D_{f_0}(u)] - \\
& - [(s-u)G_{\rho\pi\pi}^2(t)D_\rho(t) + (s-t)G_{\rho\pi\pi}^2(u)D_\rho(u)]\} = \\
& = A_{\text{box}}^2(s, t, u) + A_\epsilon^2(s, t, u) + A_{f_0}^2(s, t, u) + A_\rho^2(s, t, u);
\end{aligned}$$

The s-wave lengths of the $\pi\pi$ -scattering are defined by the formula

$$\begin{aligned}
m_\pi a_0^0 & = A^0(s = 4m_\pi^2, t = 0, u = 0) = \\
& = m_\pi [a_0^0(\text{box}) + a_0^0(\epsilon) + a_0^0(f_0) + a_0^0(\rho)], \tag{13}
\end{aligned}$$

$$\begin{aligned}
m_\pi a_2^0 & = A^2(s = 4m_\pi^2, t = 0, u = 0) = \\
& = m_\pi [a_0^2(\text{box}) + a_0^2(\epsilon) + a_0^2(f_0) + a_0^2(\rho)].
\end{aligned}$$

The phases δ_l^I of the $\pi\pi$ -scattering are defined as

$$\text{tg} \delta_l^I(s) = \text{Im} A_l^I(s) / \text{Re} A_l^I(s), \tag{14}$$

where $A_l^I(s)$ are the partial amplitudes:

$$A_l^I(s) = \frac{1}{2} \int_{-1}^1 d(\cos\theta) P_l(\cos\theta) A^I(s, t, u). \tag{15}$$

Here, θ is the scattering angle in the center of mass system, $P_l(\cos\theta)$ are the Legendre polynomials, $A^I(s, t, u)$ are defined by (10)-(12), so that

$$t = -\frac{1}{2}(s - 4m_\pi^2)(1 - \cos\theta), \quad u = -\frac{1}{2}(s - 4m_\pi^2)(1 + \cos\theta). \tag{16}$$

To obtain the imaginary part of the amplitude in our approach it is necessary to take into account the next order in the $1/N_c$ -expansion. In this work we shall restrict ourselves to the simplest way: the whole meson propagators in (8) and (9) are supposed to be got by summing up not only the diagrams in Fig.2a but also the imaginary part of the two-pion exchange ones in Fig.2b. Naturally, in this case we will get the imaginary parts only for the amplitudes with isospins $I=0,1$ because intermediate mesons with isospin $I=2$ are absent. In principle, the imaginary part of the amplitude with isospin $I=2$ can be obtained with taking into account the diagram in Fig.3. We are planning to take into account such diagrams in future. Here, we will consider only the δ_0^0 , δ_2^0 , δ_1^1 and δ_3^1 -phases.

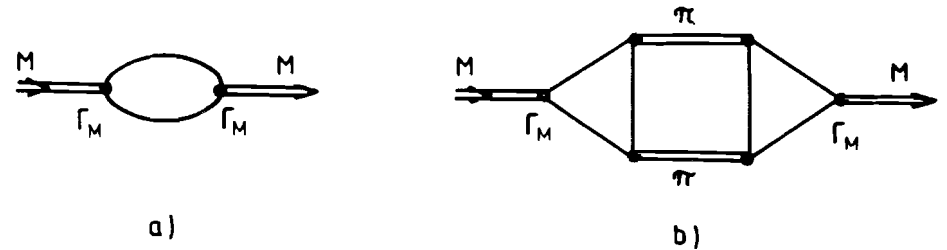


Fig.2. The diagrams defining the meson mass operator in zero (a) and first (b) orders on $1/N_c$ -expansion.

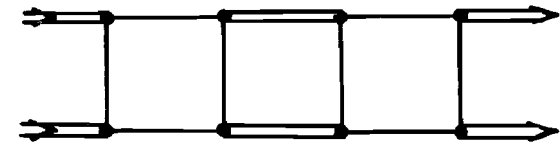


Fig.3. One of the possible diagrams defining the $\pi\pi$ -scattering in the first order on $1/N_c$ -expansion.

The imaginary part of the diagram in Fig.2b on the meson mass shell is connected with the $M \rightarrow \pi\pi$ -decay width. Therefore, we will suggest that the expressions (8) and (9) for the meson propagators off the mass shell can be generalized in the following way:

$$\tilde{D}_M(s) = \frac{1}{\Pi_M(s) - \Pi_M(m_M^2) - i\sqrt{s}\Gamma_{M \rightarrow \pi\pi}(s)}, \quad (17)$$

where $M = \rho, \epsilon, f_0$. The expressions for the widths $\Gamma_{M \rightarrow \pi\pi}$ are given in Appendix 2.

Substituting (17) into (7) and performing the algebraic transformations, we have

$$\begin{aligned} \text{Re}A_M(s, t, u) &= \frac{G_{M\pi\pi}^2(s)}{32\pi} \frac{D_M(s)}{1 + s\Gamma_{M \rightarrow \pi\pi}^2(s)D_M^2(s)}, \\ \text{Im}A_M(s, t, u) &= \frac{G_{M\pi\pi}^2(s)}{32\pi} \frac{\sqrt{s}\Gamma_{M \rightarrow \pi\pi}(s)D_M^2(s)}{1 + s\Gamma_{M \rightarrow \pi\pi}^2(s)D_M^2(s)} \end{aligned} \quad (18)$$

for $M=\epsilon$ and f_0 , respectively, and

$$\begin{aligned} \text{Re}A_\rho(s, t, u) &= \frac{(s-u)G_{\rho\pi\pi}^2(t)}{32\pi} \frac{D_\rho(t)}{1 + t\Gamma_{\rho \rightarrow \pi\pi}^2(t)D_\rho^2(t)} + \\ &+ \frac{(s-t)G_{\rho\pi\pi}^2(u)}{32\pi} \frac{D_\rho(u)}{1 + u\Gamma_{\rho \rightarrow \pi\pi}^2(u)D_\rho^2(u)}, \end{aligned} \quad (19)$$

$$\begin{aligned} \text{Im}A_\rho(s, t, u) &= \frac{(s-u)G_{\rho\pi\pi}^2(t)}{32\pi} \frac{\sqrt{t}\Gamma_{\rho \rightarrow \pi\pi}(t)D_\rho^2(t)}{1 + t\Gamma_{\rho \rightarrow \pi\pi}^2(t)D_\rho^2(t)} + \\ &+ \frac{(s-t)G_{\rho\pi\pi}^2(u)}{32\pi} \frac{\sqrt{u}\Gamma_{\rho \rightarrow \pi\pi}(u)D_\rho^2(u)}{1 + u\Gamma_{\rho \rightarrow \pi\pi}^2(u)D_\rho^2(u)}, \end{aligned} \quad (20)$$

$$\text{Re}A_{\text{box}}(s, t, u) = A_{\text{box}}(s, t, u), \quad \text{Im}A_{\text{box}}(s, t, u) = 0. \quad (21)$$

3. The scalar meson problem

The intermediate scalar mesons are very important in the $\pi\pi$ -scattering but there are some unsolved problems under their description. First, we

shall concentrate our attention on the scalar meson problem as a whole and then we shall discuss it in our approach [7].

The problem of the experimental identification of scalar mesons, the definition of their parameters and elucidating their quark structure is one of the most complicated problems in the low-energy physics. The linear realization of the chiral symmetry has required to introduce the σ -particles [11], which turned out to be convenient for the construction of the phenomenological Lagrangians reproducing the low-energy relations of the current algebra. Then, in the number of articles (see, references [1],[12] and Table 1) this fictitious meson gets the status of the physical broad ϵ -resonance which was observed in various experiments and even was included in the Particle Data Group (PDG) [12] with the mass $m_\epsilon \leq 700\text{Mev}$ and the decay width $\Gamma_\epsilon \geq 600\text{Mev}$. But, they were not included there beginning from 1974 up to now, and at present time the PDG considers that the modern experimental data can be explained without introducing the broad $\epsilon(700)$ -meson.

In our opinion, this conclusion is premature and the broad $\epsilon(700)$ -meson can be included in the PDG in future. The point is that, on the one hand, the experimental evidence of the scalar mesons, in particular $\epsilon(700)$ -meson, meets some problems (see, for example, [14]):

- 1) it is difficult to separate scalar mesons from the background and one from another because some of them are broad enough;
- 2) a number of 0^{++} -mesons, for example $f_0(975)$ and $a_0(980)$, are near inelastic thresholds and feel their strong influence;
- 3) they are smeared by the resonances with higher spins having a large statistical weight in the cross section.

On the one hand, the phenomenological analysis and model investigations of the low-energy processes permitting appearance of scalar mesons in the intermediate states indicate the importance of taking them into account in the description of the experimental data. In Table 1 there is a wide set of numerical values of m_ϵ and Γ_ϵ obtained in an analysis (see references [1],[12],[15]). One can see, the mass and decay width values are changed in a quite wide interval ($m_\epsilon = (500 - 600)\text{Mev}$ and $\Gamma_\epsilon = (300 - 1000)\text{Mev}$).

The quark composition of 0^{++} -mesons is not yet clear. The suggestion about their two-quark nature does not contradict the well-established experimental data (see, for example, [21],[22],[36]-[38]). But there are some

Table 1
The characteristics of the light broad ϵ -meson obtained
in the other models

m_ϵ (Mev)	Γ_ϵ (Mev)	Ref.; composition of ϵ -meson; computational characteristics.
≤ 700	≥ 600	[12] PDG
660 ± 100	640 ± 140	[13]
620	$\sim m_\epsilon$	[16]; $q\bar{q}$; $\Gamma_{f_0 \rightarrow \pi\pi}$
730	$\sim m_\epsilon$	[16],[17]; $q\bar{q}$; decay widths: $K \rightarrow 2\pi(3\pi)$, $\eta' \rightarrow \eta\pi\pi, \eta(\eta') \rightarrow 3\pi$; $\pi\pi$ - and KK -scattering lengths; π and K polarizabilities.
730		[18]; Dispersional relations; $\sigma_{\gamma\gamma \rightarrow \pi\pi}$, $\sigma_{\gamma\gamma \rightarrow \gamma\gamma}$.
770	~ 300	[19]; $q\bar{q}$; $\pi\pi$ -scattering lengths, $\Gamma_{a_1 \rightarrow \epsilon\pi}$, $\Gamma_{\eta \rightarrow \pi\gamma\gamma}$.
800-900	350-390	[20]; $q\bar{q}$; π and K polarizabilities.
800	1000 ± 400	[21]; $q\bar{q}$; Analysis of chiral partners of pseudoscalar mesons.
900-950		[22]; $q\bar{q}$; $\pi\pi \rightarrow \pi\pi$, $\gamma\gamma \rightarrow \pi\pi$, $pp \rightarrow ppp\pi$, $\psi \rightarrow \phi\pi\pi$, $\Upsilon' \rightarrow \Upsilon\pi\pi$.
690		[23],[24]; $\pi\pi \rightarrow \pi\pi$, $\pi K \rightarrow \pi K$, $\pi N \rightarrow \pi N$, $NN \rightarrow NN$.

phenomena, e.g. the approximate equality of the $f_0(975)$ and $a_0(975)$ meson masses, the small value of the two-photon decay width $a_0 \rightarrow \gamma\gamma$ etc. indicating a more complicated structure of scalar mesons (see, for example, [14],[35], [37], [39]-[40]). There are arguments in favour of their four-quark structure (see [13],[14],[25]-[27], [35],[39],[41]-[46]). At last, there is a number of articles, for example, [22],[27],[29]-[35], [42],[48]48-[50] where scalar mesons are assumed to be hybrid states or pure glue-

Table 1 (continuation)
The characteristics of the light broad ϵ -meson obtained
in the other models

650		[25]; $q\bar{q}q\bar{q}$; mass calculation in MIT-bag.
690		[26]; $q\bar{q}q\bar{q}$; P-matrix analysis of $\pi\pi$ - and πK -scattering phases.
645-960		[27]; $q\bar{q}q\bar{q}$ and gg ; mass calculation in MIT-bag.
750		[28]; $q\bar{q}$; mass and decay width calculation.
920	360	[29]; gg ; $J_\psi \rightarrow \gamma\pi\pi$.
~ 1000	$\sim m_\epsilon$	[22]; gg , $q\bar{q} + gg$; decay widths: $\sigma \rightarrow \pi\pi$, $S \rightarrow \gamma\gamma$, $J_\psi \rightarrow \sigma\gamma$.
850-990	380	[31]; gg ; analysis of $q\bar{q}$ and gg scalar states using low-energy theorem of broken chiral symmetry and scale invariance.
650	680	[32]; $q\bar{q} + gg$; K_{14} -decay width, s-wave phase of $\pi\pi$ -scattering.
~ 600		[33]; $q\bar{q} + gg$; $K_S \rightarrow \pi\pi$ -decay width.
500-800	500-800	[34]; $q\bar{q} + gg$; $\pi\pi \rightarrow \pi\pi$ - and $\gamma\gamma \rightarrow \pi\pi$ -scattering.
~ 800	~ 1000	[35]; $q\bar{q} + q\bar{q}q\bar{q} + gg$; $\pi\pi$ and πK -scattering.

balls. The scalar mesons (a_0, f_0, ϵ and K_0^*) were treated as two-quark states in the QCM [7]. It was found that the simplest choice of the scalar quark current as $\bar{q}\Gamma_S q$, where $\Gamma_S = I$, leads us the problem connected with that the matrix element corresponding to the strong decay $S \rightarrow \pi\pi$ becomes equal to zero at $m_S \simeq 1070$ Mev (see Fig. 4).

It leads to that a theoretical value of the $f_0(975) \rightarrow \pi\pi$ decay width is to be underestimated ($\Gamma \simeq 1$ Mev) in comparison with the experimental

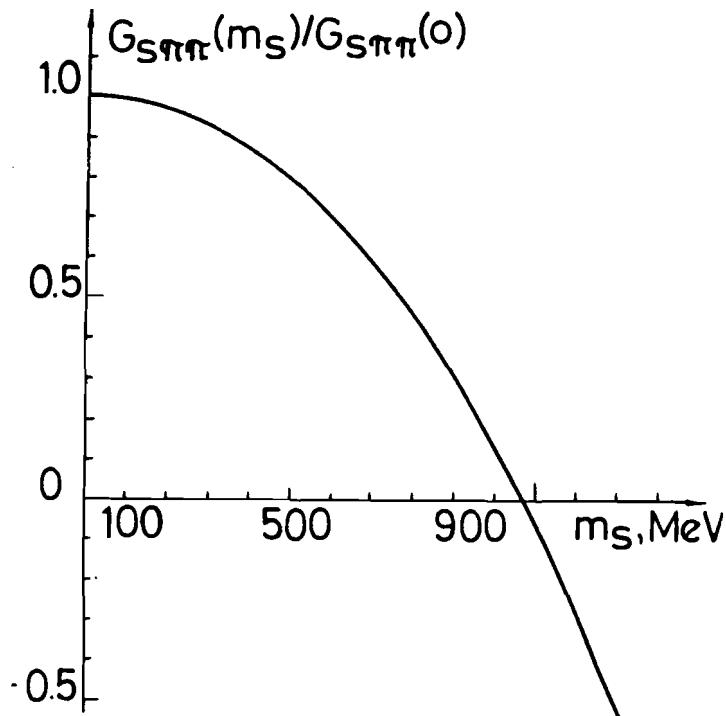


Fig. 4. The dependence of $G_{S\pi\pi}(m_S)/G_{S\pi\pi}(0)$ on mass m_S in the case $J^{0^{++}} = \bar{q}q$.

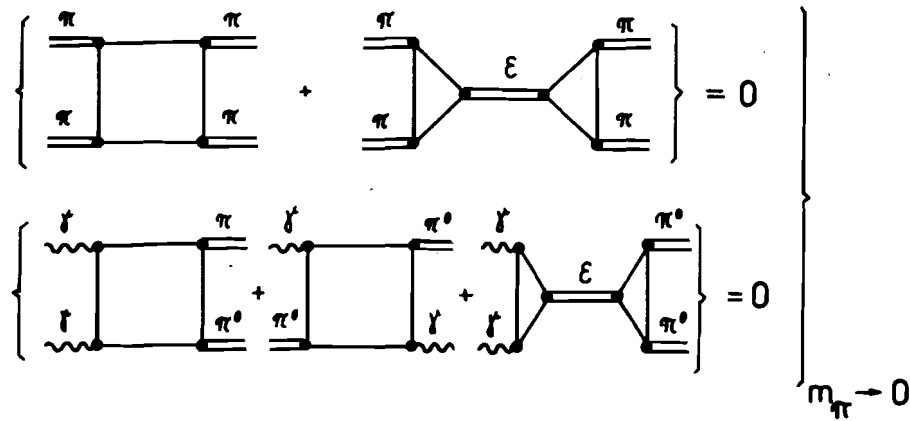


Fig. 5. The graphic condition that the $\pi\pi \rightarrow \pi\pi$ and $\gamma\gamma \rightarrow \pi\pi$ amplitudes are equal to zero when all external momenta and pion mass are equal to zero.

one ($\Gamma_{exp} = (26^{+5} \text{ Mev})$). In order to avoid this problem it was proposed to use a more complicated form of the scalar quark current with a matrix $\Gamma_S = I - iH\hat{\partial}/\Lambda$ where H was suggested to be a free parameter. The parameters H , mixing angle δ_S and mass m_ϵ have been defined by fitting, first, the experimental values of the decay $f_0 \rightarrow \pi\pi$ width, the $\pi\pi$ -scattering s-wave lengths a_0^0 and a_0^2 and, second, the condition that the amplitudes $\pi\pi \rightarrow \pi\pi$ and $\gamma\gamma \rightarrow \pi_0\pi_0$ turn to zero when both all external momenta and pion mass tend to zero (see Fig.5).

It was found that

$$H = .55; \quad \sin\delta_S = .3; \quad m_\epsilon = 600 \text{ Mev}. \quad (22)$$

Other modes of the scalar meson decays, the pion polarizabilities and nonleptonic kaon decays, were described with quite a good accuracy using these values [7].

4. The $\pi\pi$ -scattering phase shifts

As has been mentioned above the main aim of this work is to describe more sophisticated characteristics of the $\pi\pi$ -scattering as phase shifts. As a rule, the most considerable efforts are applied to explain the behaviour of the lowest δ_0^0 -phase because this is very sensitive to a change of model parameters.

Therefore, we first calculate the A_0^0 -amplitude using the obtained values of the scalar meson parameters (22). Separate contributions from every diagram and the total result for the ReA_0^0 are shown in Fig.6. One can see, our curve turns to zero at $M_{\pi\pi} \simeq m_\epsilon = 600 \text{ Mev}$ which is due to the presence of the light ϵ -meson in our approach. But the experimental curve turns to zero at $M_{\pi\pi} \simeq 750 - 900 \text{ Mev}$.

Thus, the question is whether it is possible to describe both the s-wave lengths and phase in our approach from the unique point of view. To answer this question we will perform a new fit to experimental data including the s-wave phase and suggesting that the scalar meson parameters H , δ_S and m_ϵ are free.

Table 2
The s-wave $\pi\pi$ -scattering lengths
(a) Separate contributions

QCM	a_0^0	a_0^2
$b\omega$	-1.10	-0.440
ϵ	1.19	0.432
f_0	0.02	0.007
ρ	0.12	-0.062
<i>total</i>	0.23	-0.063

Table 2 (continuation)
The s-wave $\pi\pi$ -scattering lengths
(b) Other approaches.

Method	a_0^0	a_0^2
QCM	0.23	-0.06
Experiment [2],[60]	0.23 ± 0.05	-0.05 ± 0.03
Chiral Lagrangians [60]	0.22	-0.05
Superconductive model [16]	0.26	-0.05
Current algebra [61]	0.20	-0.06

First of all, let us make some remarks about a sensitivity of the physical values on these parameters. Formally the a_0^0 and a_0^2 depend on H , $\sin\delta_S$ and m_ϵ but really they are not sensitive to a change of $\sin\delta_S$. The dependence on H is much stronger than on m_ϵ so that one can find such a value of H for any m_ϵ to describe a_0^0 and a_0^2 simultaneously. In fact, a passage of the phase δ_0^0 through $\frac{\pi}{2}$ is defined by a value of m_ϵ .

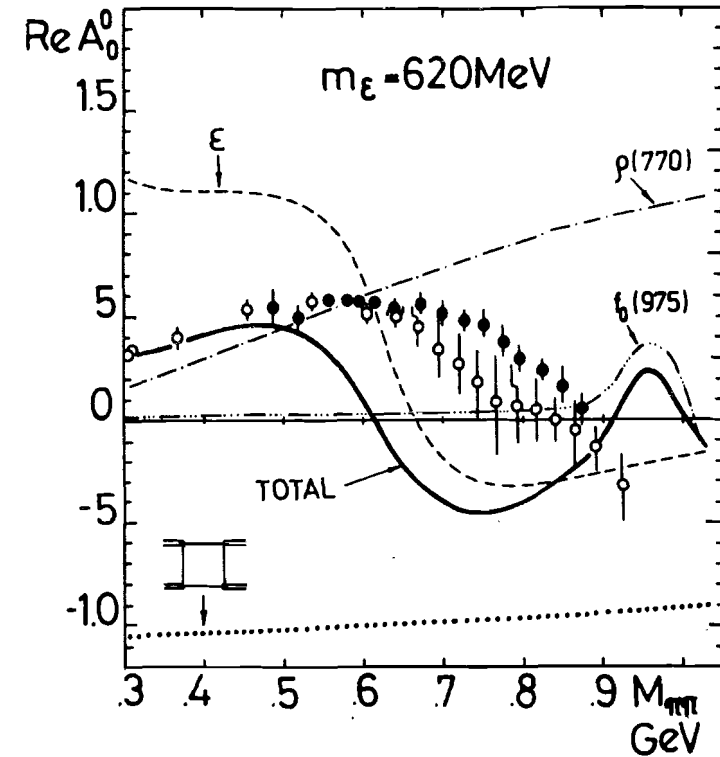


Fig.6. The dependence of $Re A_0^0$ on $M_{\pi\pi}$. The experimental data are from [51] and [52].

Therefore, we use the following scheme of fitting:

- 1) One calculates a_0^0 and a_0^2 for different values of m_ϵ and plots them as functions of H (see Fig.7). After that, one defines the allowed connection of H and m_ϵ (see Fig.9) from the best agreement with experimental data.
- 2) One calculates $\Gamma_{f_0 \rightarrow \pi\pi}$ for different values of H and plots it as a function of $\sin\delta_S$ (see Fig.7). After that, one defines the allowed connection of H and $\sin\delta_S$ (see Fig.9) from the best agreement with experimental data.
- 3) One calculates δ_0^0 for different values of m_ϵ using the obtained values of H and δ_S and plots it as a function of $M_{\pi\pi}$ (see Fig.10). After that, one defines m_ϵ from the best agreement with experimental data.

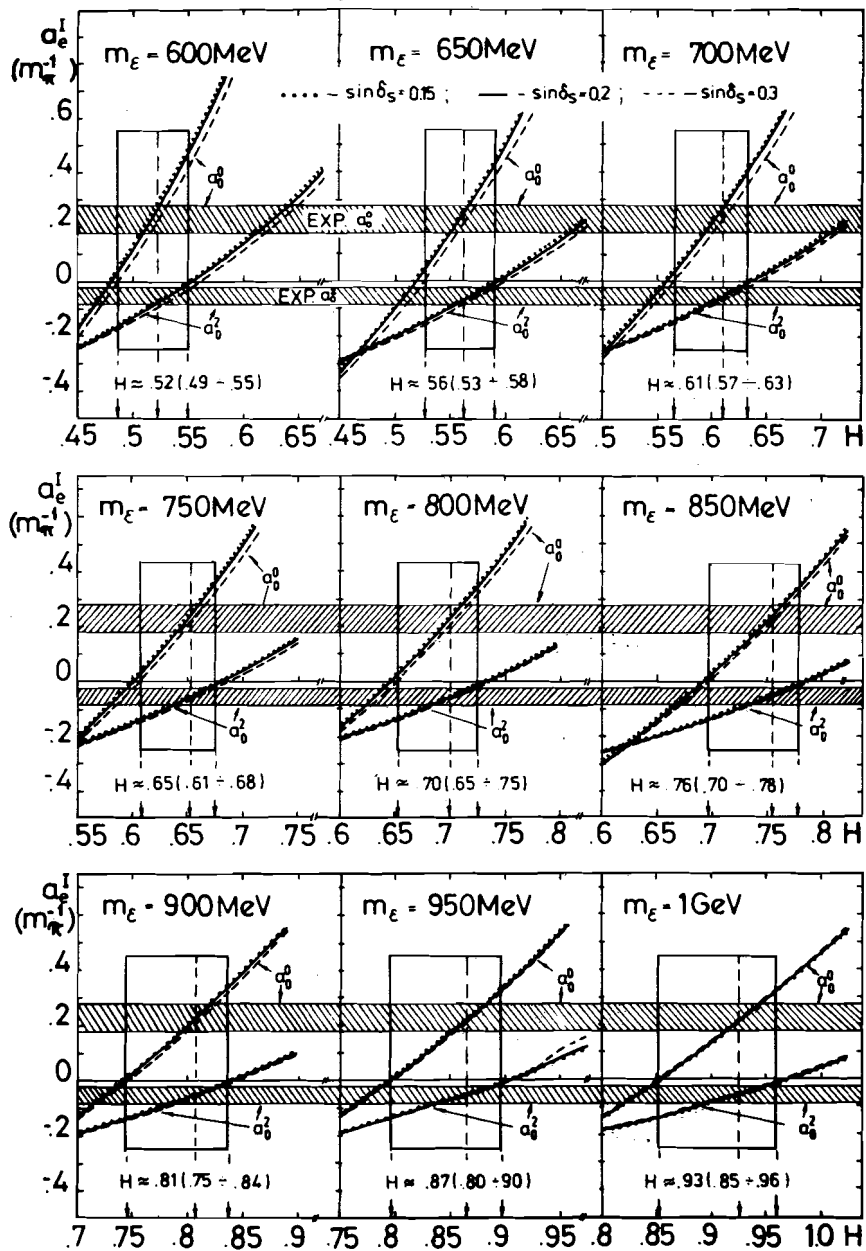


Fig.7. The fitting of parameters H and m_ϵ to experimental data of a_0^0 and a_0^2 .

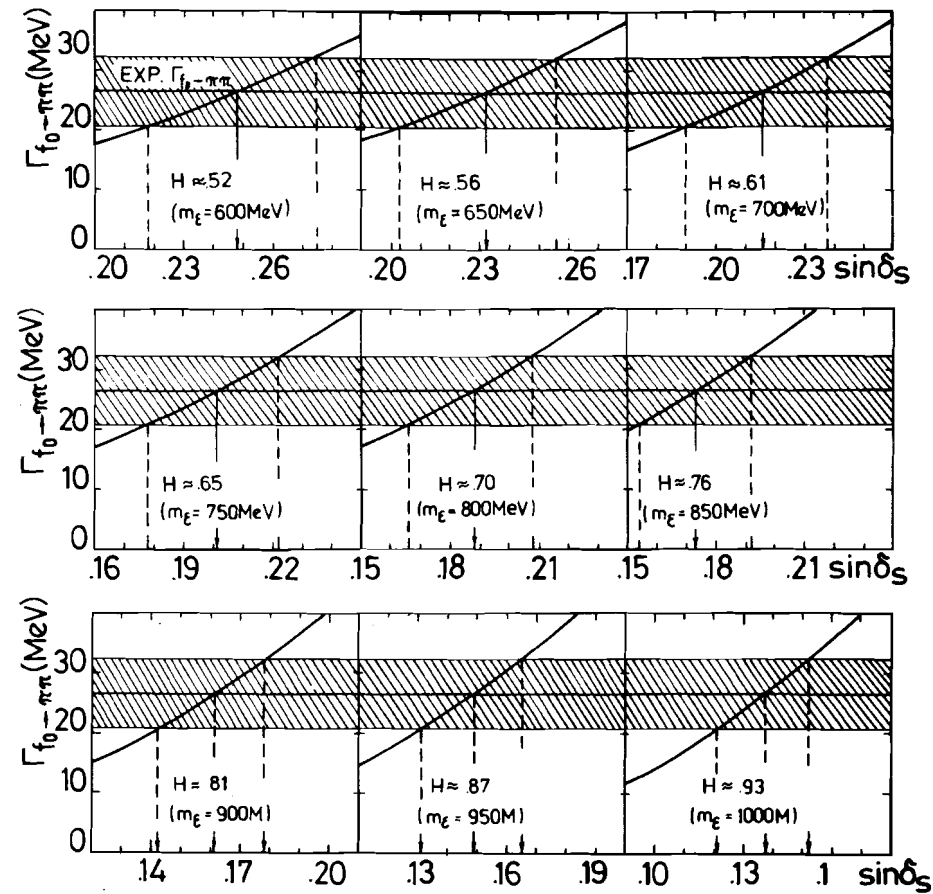


Fig.8. The fitting of parameters $\sin\delta_S$ and m_ϵ (or H) to experimental data of $\Gamma_{f_0 \rightarrow \pi\pi}$.

The best agreement with experimental data for a_0^0 , a_0^2 , $\Gamma_{f_0 \rightarrow \pi\pi}$ and δ_0^0 simultaneously is achieved when

$$m_\epsilon \in (700 - 800) \text{ Mev} \quad H \in (.57 - .77) \quad \sin\delta_S \in (.17 - .24)$$

The s-wave phase δ_0^0 is described in our approach with a satisfactory accuracy up to $M_{\pi\pi} \simeq 900$ Mev with taking into account the ϵ -meson

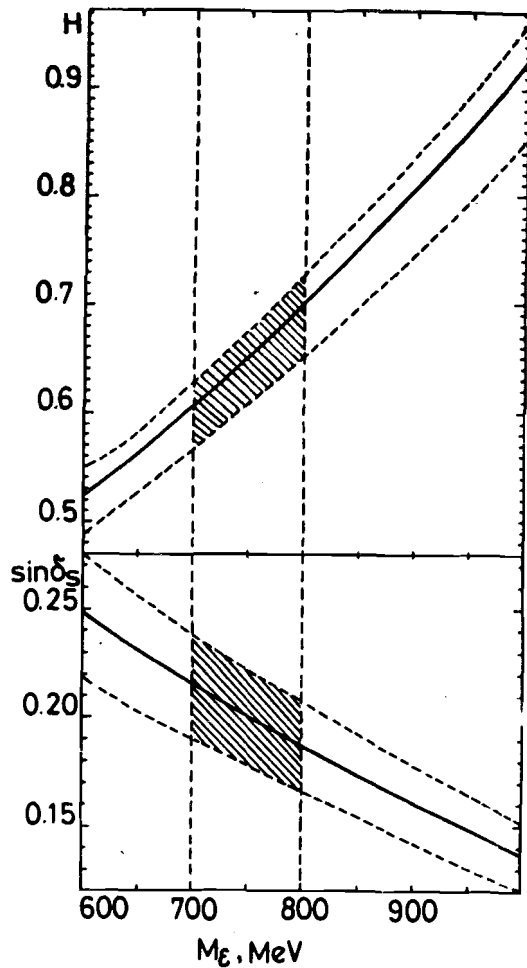


Fig.9. The allowed interval of values m_ϵ and H .

with mass $m_\epsilon \simeq 700 - 800$ Mev. The fall of the theoretical curve δ_0^0 near $M_{\pi\pi} \simeq 950$ Mev is caused by the narrow shape of the $f_0(975)$ -resonance having $\Gamma_{total} \simeq 26$ Mev (see Fig.6). To describe behaviour of the δ_0^0 above 950 Mev it is need to take into account the coupling of the $f_0(975)$ with the $K\bar{K}$ -channel and also the contribution of higher resonances.

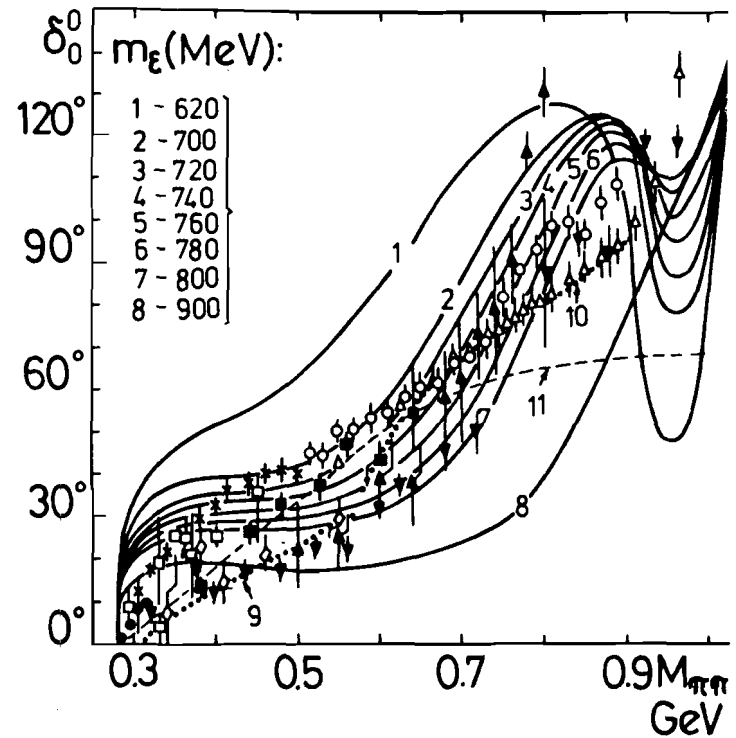


Fig.10. The dependence of δ_0^0 on $M_{\pi\pi}$. The solid lines (1)-(8) are our results for the different values of m_ϵ indicating here. The lines (9), (10) and (11) are from [32], [23] and [59], respectively. The experimental data are from [53]-[58]

The numerical values of the s-wave lengths a_0^0 and a_2^0 are shown in Table 2. There are separate contributions from every diagram and total results. One can see, there is a good agreement of our results with experimental data [2],[60] and other approaches.

The dependence of the $\epsilon \rightarrow \pi\pi$ decay width on the ϵ -meson mass is shown in Fig.11. One can see that $\Gamma_{\epsilon \rightarrow \pi\pi} \in (700 - 930)$ Mev in the allowed interval of free parameters (22). In other words, the scalar ϵ -meson turns out to be broad enough in our approach.

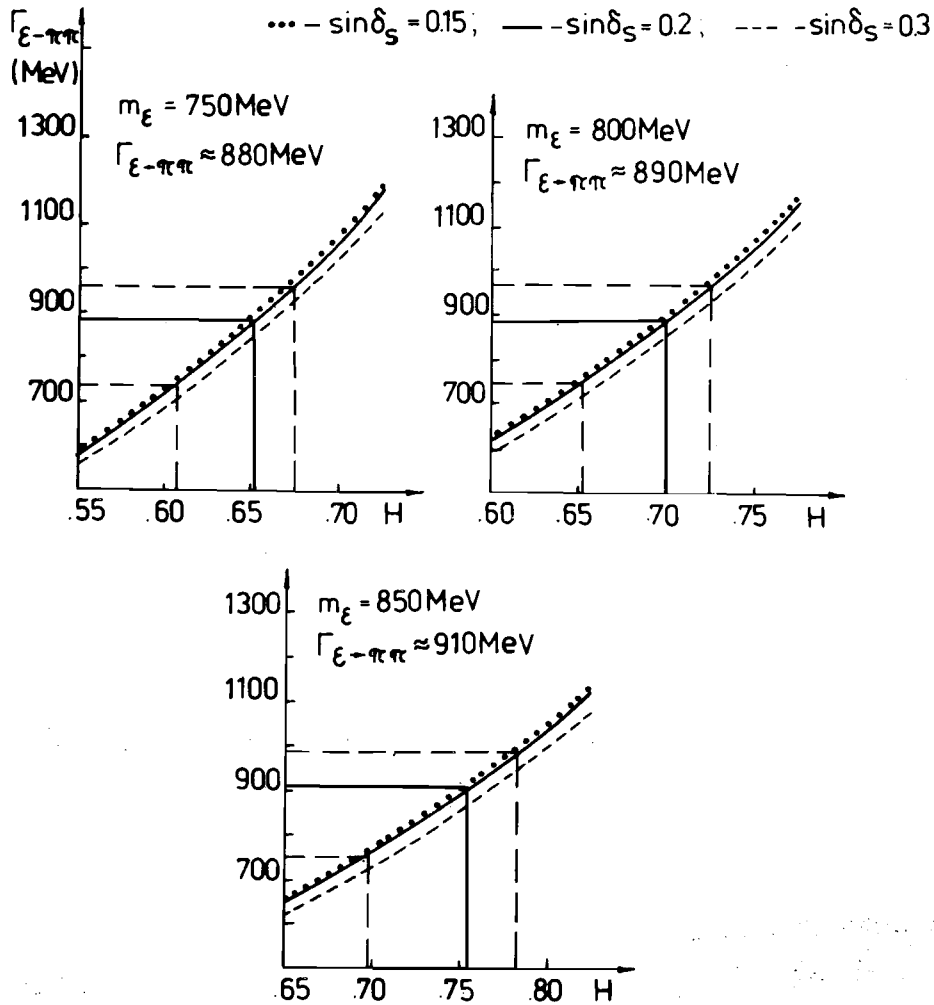


Fig.11. The dependence of $\Gamma_{\epsilon \rightarrow \pi\pi}$ on H .

We have obtained also the behaviour of the higher phases δ_1^1 , δ_3^1 and δ_2^0 using the above fixed parameters (see Fig.12,13). The behaviour of δ_1^1 and δ_3^1 is completely defined by the ρ -meson exchange. The magnitudes of δ_1^1 and δ_3^1 are small up to $M_{\pi\pi} < 1$ Gev. Therefore, the theoretical values of δ_1^1, δ_2^0 and δ_3^1 are not sensitive to a change of scalar meson parameters up to $M_{\pi\pi} \simeq 900$ Mev.

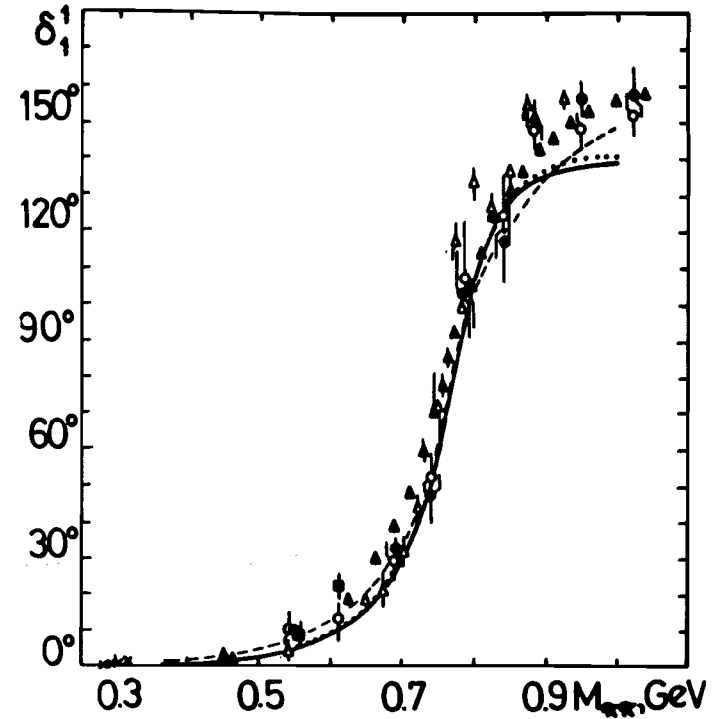


Fig.12. The dependence δ_1^1 on $M_{\pi\pi}$. The solid line is our result. The point line is the ρ -meson contribution only. The dash line is result from [59]. The experimental data are from [62]-[64].

4. Summary and outlook

Thus, the s-wave lengths and phases of $\pi\pi$ -scattering and the two-pion decay widths of scalar mesons are simultaneously described in the framework of the QCM. It was found that the broad $\epsilon(700 - 800)$ -meson with $\Gamma_{\epsilon \rightarrow \pi\pi} \geq M_\epsilon$ must be taken into account and this conclusion is believed to be model independent.

We consider our results as preliminary ones. Further we are going to perform more careful calculation of the $\pi\pi$ -scattering amplitude in the first order of the $1/N_c$ -expansion. It is interesting to investigate scalar mesons as more complicated objects like four-quark states or mixture of quark and gluon ones. Moreover, it is necessary to consider other

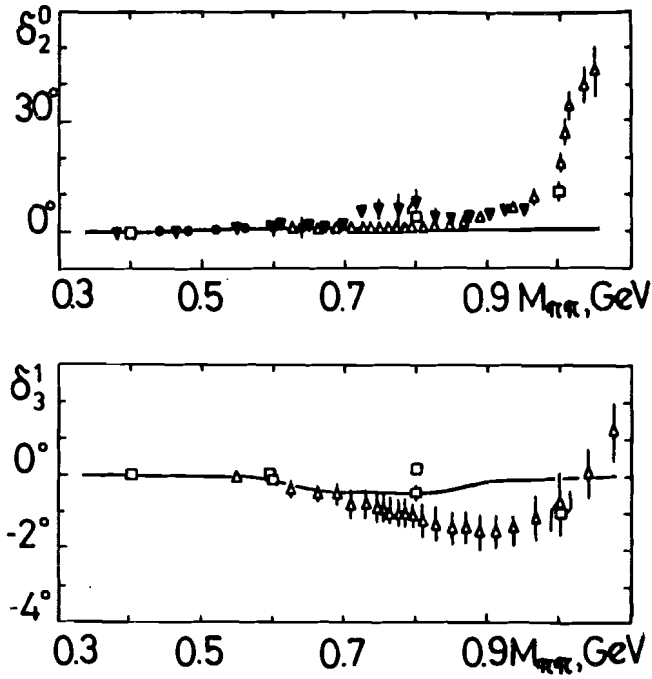


Fig.13. The dependence of δ_2^0 and δ_3^1 of $M_{\pi\pi}$. The solid lines are our results. The experimental data are from [55],[64],[65].

processes with scalar mesons in intermediate states, for example, $\pi N \rightarrow \pi N$; $NN \rightarrow NN$; $\gamma\gamma \rightarrow \pi\pi$; $N\bar{N} \rightarrow \pi\pi$; $\eta' \rightarrow \eta\pi\pi$; $\eta(\eta') \rightarrow 3\pi$; $K \rightarrow 2\pi, 3\pi$ etc.

At last, undoubtedly more reliable experimental data on scalar meson characteristics are needed to clarify the nature of scalar mesons and their role in the low-energy physics.

Acknowledgments

We would like to thank R.Arndt, N.N.Achasov, S.B.Gerasimov, A.B.Govorkov, G.Holler, M.Hooper, J.Lanik, E.P.Shabalin and M.K.Volkov for the fruitful discussions of the problems considered in this work.

Appendix 1

The effective coupling constants h_M are determined from (5) using the QCM calculation methods [5]:

$$h_\pi = \frac{2}{F_{PP}(x_\pi)} = 0.863;$$

$$h_\rho = \frac{3}{F_{VV}(x_\rho)} = 0.798.$$

$$h_{f_0} = \frac{2}{F_{SS}(x_{f_0})\sin^2\delta_S + F_{SS}(y_{f_0})\cos^2\delta_S} = 0.39,$$

$$h_\epsilon = \frac{2}{F_{SS}(x_\epsilon)\cos^2\delta_S + F_{SS}(y_\epsilon)\sin^2\delta_S} = 0.88,$$

when $H = 0.55$; $\sin\delta_S = 0.24$.

Here

$$F_{PP}(x) = C_B^{(0)} + \frac{x}{4} \int_0^1 du b\left(-\frac{ux}{4}\right) \left(1 - \frac{u}{2}\right) / \sqrt{1-u},$$

$$F_{VV}(x) = C_B^{(0)} + \frac{x}{4} \int_0^1 du b\left(-\frac{ux}{4}\right) \left(1 - \frac{u}{2} + \frac{u^2}{4}\right) / \sqrt{1-u},$$

$$F_{SS}(x) = F_{SS}^{(0)}(x) + 4H F_{SS}^{(1)}(x) - 4H^2 F_{SS}^{(2)}(x)$$

$$F_{SS}^{(0)}(x) = C_B^{(0)} + \frac{x}{4} \int_0^1 du b\left(-\frac{ux}{4}\right) \left(1 + \frac{u}{2}\right) \sqrt{1-u},$$

$$F_{SS}^{(1)}(x) = C_A^{(0)} + \frac{x}{4} \int_0^1 du a\left(-\frac{ux}{4}\right) \left(1 + \frac{u}{2}\right) \sqrt{1-u},$$

$$F_{SS}^{(2)}(x) = C_B^{(1)} + \frac{x}{4} \int_0^1 du b\left(-\frac{ux}{4}\right) u \left(1 + \frac{u}{2}\right) \sqrt{1-u}.$$

In the present work all the calculations of the physical matrix elements were performed with inclusion of mass dependences. But it turned out that the obtained values depend very slightly on the pion mass. Therefore, we present below the expressions of structure integrals without the pion mass.

1. $\rho \rightarrow \pi\pi$

$$\Gamma_{\rho\pi\pi}(m_\rho^2) = \frac{m_\rho^2}{48\pi} \left(1 - \frac{4m_\pi^2}{m_\rho^2}\right)^{\frac{3}{2}} g_{\rho\pi\pi}^2(m_\rho^2),$$

$$g_{\rho\pi\pi}(m_\rho^2) = \frac{2\pi}{\sqrt{6}} h_\pi \sqrt{h_\rho} F_{VPP}(x_\rho), \quad G_{\rho\pi\pi}(s) \equiv \frac{g_{\rho\pi\pi}}{\sqrt{h_\rho}},$$

$$F_{VPP}(x) = C_B^{(0)} + \frac{x}{4} \int_0^1 du b\left(-\frac{ux}{4}\right) \sqrt{1-u}.$$

2. $S \rightarrow \pi\pi$

$$\Gamma_{S\pi\pi}(m_S^2) = \frac{3}{32\pi} \sqrt{\left(1 - \frac{4m_\pi^2}{m_S^2}\right)} \frac{g_{S\pi\pi}^2(m_S^2)}{m_S},$$

$$g_{S\pi\pi}(m_S^2) = \pi \Lambda h_\pi \sqrt{\frac{h_S}{6}} F_{SPP}(x_S) C_{SPP}, \quad G_{S\pi\pi}(s) \equiv \frac{g_{S\pi\pi}}{\sqrt{h_S}},$$

$$C_{f_0\pi\pi} = -4\sin\delta_S \quad C_{\epsilon\pi\pi} = 4\cos\delta_S,$$

$$F_{SPP}(x) = F_{SPP}^{(0)}(x) - 4H F_{SPP}^{(1)}(x),$$

$$F_{SPP}^{(0)}(x) = C_A^{(0)} - \frac{x}{4} \int_0^1 du a\left(-\frac{ux}{4}\right) \left[\frac{1}{2} \ln \frac{1 + \sqrt{1-u}}{1 - \sqrt{1-u}} - \sqrt{1-u}\right],$$

$$F_{SPP}^{(1)}(x) = C_B^{(1)} - \frac{x^2}{32} \int_0^1 du b\left(-\frac{ux}{4}\right) u \left[\frac{1}{2} \ln \frac{1 + \sqrt{1-u}}{1 - \sqrt{1-u}} - \sqrt{1-u}\right].$$

$$\begin{aligned} G_{\text{box}}(s, t, u) = & \\ = & \frac{4\pi^2}{3} h_\pi^2 \left\{ C_B^{(0)} - \frac{t}{8\Lambda^2} \int_0^1 dx b\left(-\frac{xt}{4\Lambda^2}\right) \left[\ln \frac{1 + \sqrt{1-x}}{1 - \sqrt{1-x}} - \sqrt{1-x} \right] - \right. \\ & \left. - \frac{s}{8\Lambda^2} \int_0^1 dx b\left(-\frac{xs}{4\Lambda^2}\right) \left[\ln \frac{1 + \sqrt{1-x}}{1 - \sqrt{1-x}} - \sqrt{1-x} \right] - \right. \\ & \left. - \frac{su}{2\Lambda^4} \int_0^1 dx \int_0^{1-x} dy \int_0^{1-x-y} dz z b' \left[-\frac{xzs + yt(1-x-y-z)}{\Lambda^2} \right] \right\}, \end{aligned}$$

$$\begin{aligned} R(x) = & C_B^{(0)} + \frac{x}{4} \int_0^1 du b(-xu/4) (1-u)^{\frac{3}{2}} + \\ & + 4H \left[C_A^{(0)} + \frac{x}{4} \int_0^1 du a(-xu/4) (1-u)^{\frac{3}{2}} \right] - \\ & - 4H^2 \left[C_B^{(1)} - \left(\frac{x}{4}\right)^2 \int_0^1 du b(-xu/4) (1-u)^{\frac{3}{2}} u \right]. \end{aligned}$$

$$B_0(x) = C_B^{(0)} + \frac{x}{4} \int_0^1 du b(-xu/4) \sqrt{1-u} \left(1 + \frac{x}{2}\right).$$

References

- [1] B.R.Martin et al., Pion-pion interactions in particle physics, N.Y., "Academic Press", 1976.
- [2] A.A.Bel'kov et al., Pion-pion interaction, M., "Energoatomizdat", 1985.
- [3] G.A.Leksin, Usp.Fiz.Nauk, 1970, v.102, 387.
- [4] K.N.Muhin, O.O.Patarakin, Usp.Fiz.Nauk, 1981, v.133, 377.

- [5] G.V.Efimov, M.A. Ivanov, Inter.Jour.of Mod.Phys., 1989, A4, 2031.
- [6] E.Z.Avakyan et al., Yad.Fiz., 1987, v.46, 576; JINR, E2-87-630, Dubna, 1987.
- [7] E.Z.Avakyan et al., Yad.Fiz., 1989, v.49, 1398.
- [8] G.V.Efimov, M.A.Ivanov, V.E.Luboviskij, Few-Body Systems, 1989, v.6, 17.
- [9] G.V.Efimov, M.A.Ivanov, S.G.Mashnik, JINR, P2-88-253, Dubna, 1988.
- [10] K.Hayashi et al., Fort. der Phys., 1967, v.15, 625.
- [11] V.De Alfaro et al., Currents in Hadron Physics, North-Holland Publishing Company, Amsterdam-London, 1973.
- [12] Partile Data Group, Phys.Lett., 1972, B39, 1; Phys.Lett., 1974, B50, 1.
- [13] F.E.Close, An Introduction To Quarks And Partons, Academic Press, London-New-York-San-Francisco, 1979.
- [14] N.N.Achasov, S.A.Devyanin, G.N.Shestakov, Usp.Fiz.Nauk, 1984, v.142,361.
- [15] Partile Data Group, Phys.Lett., 1988, B204, 1.
- [16] M.K.Volkov, Particles and Fields, 1986, v.17, 433.
- [17] M.K.Volkov, Ann. of Phys., 1983, v.157, 282; D.Ebert, Volkov M.K., Z.fur Phys., 1983, C16, 205; M.K.Volkov, A.A.Osipov, Yad.Fiz., 1984, v.39, 694; M.K.Volkov, A.N.Ivanov, N.I.Troitskaya, Yad.Fiz., 1988, v.47, 1157.
- [18] P.S.Isaev, V.I.Hlestakov, Yad.Fiz., 1972, v.12, 1012.
- [19] M.K.Volkov, JINR, P2-338, Dubna, 1982; M.K.Volkov, D.V.Kreopalov, Yad.Fiz., 1983, v.37, 1297; M.K.Volkov, A.A.Osipov, Yad.Fiz., 1984, v.39, 694.
- [20] M.K.Volkov, A.A.Osipov, JINR, E2-83-921, Dubna, 1984.
- [21] E.P.Shabalin, Yad.Fiz., 1984, v.40, 262.
- [22] K.L.Au, D.Morgan, M.R.Penington, Phys.Lett., 1986, B167, 229; Phys.Rev., 1987, D35, 1633.
- [23] I.M.Narodetskii, In: "Nucleon-nucleon interactions and hadron-nuclear interactions at the intermediate energy", LINR, 1986.
- [24] I.M.Narodetskii, Proc. 10 Europ. Symp. on Dynamics of Few-Body System, Balatonfureed, 23, 1985; I.L.Grach, Yu.S.Kalashnikova, I.M.Narodetskii, Yad.Fiz., 1987, v.45, 1428; A.I.Veselov et al., Yad.Fiz., 1988, v.47, 21; I.L.Grach, I.M.Narodetskii, Yad.Fiz., 1987, v.46, 1038; I.L.Grach, Yu.S.Kalashnikova, Yad.Fiz., 1987, v.46, 1619.
- [25] R.L.Jaffe, Phys.Rev., 1977, D15, 267; 1977, D15, 281.
- [26] R.L.Jaffe, F.E.Low, Phys.Rev., 1979, D19, 2105.
- [27] R.L.Jaffe, K.Johnson, Phys.Lett., 1975, B60, 201.
- [28] M.K.Volkov, D.V.Kreopalov, Yad.Fiz., 1984, v.39, 924; Teor.Mat.Fiz, 1983, v.57, 21.
- [29] J.Lanik, K.Safarik, JINR, E2-88-465, Dubna, 1988.
- [30] J.Ellis, J.Lanik, Phys.Lett., 1986, B175, 83.
- [31] J.Lanik, Z.fur Phys., 1988, C39, 143.
- [32] E.P.Shabalin, Yad.Fiz., 1989, v.49, 588.
- [33] E.P.Shabalin, Yad.Fiz., 1988, v.48, 272; 1988, v.48, 1357.
- [34] G.Menessier, S.Narison, N.Pauer, Phys.Lett., 1985, B158, 153; G.Menessier, Z.fur Phys. 1983, C16, 241.
- [35] P.Estarbrooks, Phys.Rev., 1979, D19, 2678.
- [36] T.De Grand et al., Phys.Rev., 1975, D19, 2678.
- [37] A.T.Philipov, Usp.Fiz.Nauk, 1982, v.137, 201.
- [38] E.P.Shabalin, Yad.Fiz., 1985, v.42, 260.

- [39] T.Barnes, Phys.Lett., 1985, B165, 434.
- [40] A.D.Martin, E.N.Ozmutlu, E.J.Squires, Nucl.Phys., 1977, B121, 514.
- [41] N.N.Achasov, S.A.Devyanin, G.N.Shestakov, Yad.Fiz., 1980, v.32, 1098; 1981, v.33, 1337.
- [42] Sh.S.Eremyan, A.E.Nazaryan, Yad.Fiz., 1987, v.46, 1774; 1986, v.43, 1303.
- [43] S.Narison, Phys.Lett., 1986, B175, 88.
- [44] N.A.Tornqvist, Phys.Rev.Lett., 1982, v.49, 624.
- [45] S.G.Godfrey, N.Isgur, Phys.Rev., 1985, v.D32, 189; M.Frank et al., Phys.Rev., 1985, D32, 2971.
- [46] J.Weinstein, N.Isgur, Phys.Rev.Lett., 1982, v.48, 659; Phys.Rev., 1983, D27, 588.
- [47] O.Sh.Rasizade, Yad.Fiz., 1980, v.31, 725.
- [48] I.Yu.Kobzarev, B.V.Martemyanov, M.G.Schepkin, Pizma JETPh, 1977, v.25, 600.
- [49] A.I.Vainshtein et al., Particles and Fields, 1982, v.13, 542.
- [50] J.Govaers et al., Phys.Lett., 1983, B128, 262.
- [51] E.A.Alekseeva et al., Yad.Fiz., 1982, v.35, 917.
- [52] N.N.Biswas et al., Phys.Rev.Lett., 1981, v.47, 1378; N.M.Cason et al., Phys.Rev., 1983, D28, 1586.
- [53] V.Hagopian et al., in: "Proc. Conf. on $\pi\pi$ and KK Interac.", Aragonne National Laboratory, 1969, p.149.
- [54] P.Estarbrooks, A.Martin, Nucl.Phys., 1974, B79, 301.
- [55] V.Srinivasan et al., Phys.Rev., 1975, D12, 681.
- [56] A.A.Bel'kov et al., Pizma JETPH, 1979, v.29, 652.
- [57] M.M.Makarov et al., Yad.Fiz., 1970, v.11, 608.
- [58] L.Rosselet et al., Phys.Rev., 1974, D15, 574.
- [59] M.K.Volkov, V.N.Pervushin, Nuovo Cim., 1975, A27, 277.
- [60] A.A.Bel'kov, V.N.Pervushin, D.Ebert, JINR, P2-88-656, Dubna, 1988.
- [61] S.Weinberg, Phys.Rev.Lett., 1966, v.17, 616.
- [62] E.A.Alekseeva et al., JETPH, 1982, v.82, 1007.
- [63] A.A.Bel'kov et al., Pizma JETPH, 1982, v.29, 652.
- [64] S.D.Protopopescu et al., Phys.Rev., 1973, D7, 1279.
- [65] J.L.Basdevant et al., Nucl.Phys., 1974, B72, 413.
- [66] A.E.Dorokhov A.E., Yu.A.Zubov, N.I.Kochelev, JINR, E2-89-235, Dubna, 1989.

Received by Publishing Department
on November 17, 1989.